10558 *Biochemistry* **2009,** *48,* 10558–10567
DOI: 10.1021/bi901462e

BIOCHEMISTRY
including biophysical chemistry & molecular biology
Article

Structural Basis for the Lack of E2 Interaction in the RING Domain of TRAF2[†]

Qian Yin,[‡] Betty Lamothe,[§] Bryant G. Darnay,[§] and Hao Wu*[,‡]

[‡]*Weill Medical College of Cornell University, New York, New York 10021, and* [§]*Department of Experimental Therapeutics, University of Texas M. D. Anderson Cancer Center, Houston, Texas 77030*

Received August 20, 2009; Revised Manuscript Received October 6, 2009

ABSTRACT: TRAF proteins are intracellular signal transducers for a number of immune receptor superfamilies. Specifically, TRAF2 interacts with members of the TNF receptor superfamily and connects the receptors to downstream signaling proteins. It has been assumed that TRAF2 is a ubiquitin ligase like TRAF6 and mediates K63-linked polyubiquitination of RIP1, a kinase pivotal in TNFα-induced NF-κB activation. Here we report the crystal structure of the RING and the first zinc finger domains of TRAF2. We show that the TRAF2 RING structure is very different from the known TRAF6 RING structure. The differences are multifaceted, including amino acid differences at the critical Ubc13-interacting site, local conformational differences, and a unique nine-residue insertion between the RING domain and the first zinc finger in TRAF2. These structural differences prevent TRAF2 from interacting with Ubc13 and other related E2s via steric clash and unfavorable interfaces. Our structural observation should prompt a re-evaluation of the role of TRAF2 in TNFα signaling and may indicate that TRAF2-associated proteins such as cIAPs may be the ubiquitin ligases for NF-κB signaling.

TRAF2 is a RING domain-containing protein that was first identified from biochemical purification as a TNFR2-associated signaling protein (*1*). It interacts with many receptors in the TNF receptor superfamily and mediates the survival effects of these receptors (*2*, *3*). The TRAF family now consists of seven mammalian members and is shown to participate in signal transduction of a large number of receptor families that also include the IL-1 receptors (IL-1R), the Toll-like receptors (TLR), T-cell receptors (TCR), and B-cell receptors (BCR) (*4*, *5*). Upon receptor activation, TRAFs are directly or indirectly recruited to the intracellular domains of these receptors. They subsequently engage other signaling proteins to activate the inhibitor of κB (IκB) kinase (IKK) and MAP kinases, leading ultimately to activation of transcription factors such as NF-κB and AP-1 to induce immune and inflammatory responses and confer protection from apoptosis.

Like most TRAFs, TRAF2 contains an N-terminal domain with a RING domain and four zinc fingers and a C-terminal TRAF domain that comprises a coiled coil domain and a conserved TRAF-C domain (*1*) (Figure 1A). Previous biochemical and structural studies have revealed that the TRAF domain forms a mushroom-shaped trimeric structure with the TRAF-C domain as the head for interaction with receptors and adaptor proteins and the coiled coil domain as the stalk for trimerization (*6*−*10*). The receptor-binding groove of TRAF2 is similar in sequence and structure with those of TRAF1, -3, and -5 but is dissimilar to that of TRAF6.

TRAF proteins were originally considered adapter proteins that connect activated receptors to downstream kinases for signal amplification. However, it was then shown that TRAFs might be RING-type ubiquitin ligases. This has been shown for TRAF6, which catalyzes K63-linked polyubiquitination both in vitro and in cells (*11*). Unlike K48-linked polyubiquitin chains that are hallmarks for proteasomal degradation, the K63 linkage is nondegradative and has been discovered to function as a signaling moiety in DNA damage repair processes and innate immunity pathways (*12*, *13*). Ubiquitination is accomplished in three steps, ATP-dependent attachment of ubiquitin to a ubiquitin activating enzyme (E1), transfer of ubiquitin from E1 to a ubiquitin conjugating enzyme (E2), and transfer of ubiquitin from E2 to Lys residues of substrates with the aid of a ubiquitin ligase (E3) (*12*, *14*, *15*).

Upon activation by the relevant signaling pathways after ligand stimulation, TRAF6 promotes K63-linked polyubiquitination of itself and downstream signaling proteins, a process that requires the heterodimeric E2 of Ubc13 and the ubiquitin E2 variant (Uev) known as Uev1A (*12*). The K63-linked polyubiquitin chains function as anchors to recruit the TAK1 kinase complex and IKK to activate both the MAP kinase pathway and the NF-κB pathway (*16*, *17*). TAK1 directly phosphorylates MAP kinases, while IKK-mediated phosphorylation of IκB leads to its degradation to free NF-κB for transcription.

It has been implied that TRAF2 may act like TRAF6 in stimulating K63-linked polyubiquitination in the TNFα and other related pathways. An assumed concept is that TRAF2 mediates K63-linked ubiquitination of RIP1, a kinase pivotal in TNFα-induced NF-κB activation (*18*). Here we show, however, that the TRAF2 RING structure is very different from the TRAF6 RING structure we determined previously (*19*). The differences are due to multiple changes between TRAF2 and TRAF6, including amino acid differences at the critical Ubc13 interacting site, conformational differences, and a unique nine-residue insertion between the RING domain and the first

[†]This work was supported by the National Institutes of Health (Grant RO1 AI045937 to H.W. and Grant RO1 AR053540 to B.G.D.) and institutional start-up funds to B.G.D.

*To whom correspondence should be addressed: Department of Biochemistry, Weill Medical College of Cornell University, 1300 York Ave., New York, NY 10021. Phone: (212) 746-6451. Fax: (212) 746-4843. E-mail: haowu@med.cornell.edu.

 Published on Web 10/07/2009

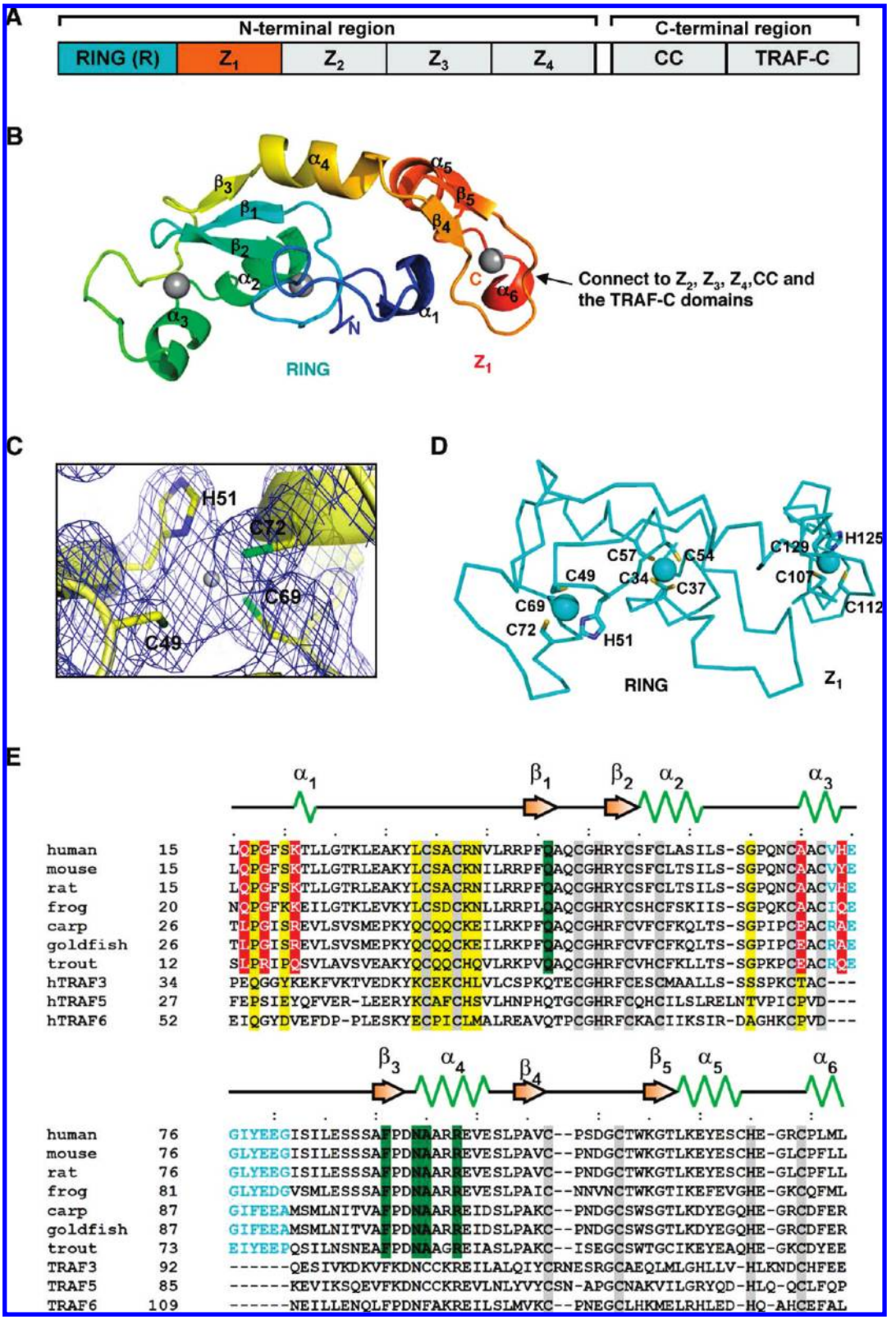

FIGURE 1: Structure of the human TRAF2 RING and first zinc finger domains (RZ_1). (A) Domain organization of TRAF2. Z_1-Z_4 are zinc finger domains 1−4, respectively, and CC is the coiled coil domain. (B) Ribbon diagram of TRAF2 RZ_1 colored in a rainbow mode from the N- to C-terminus. Secondary structure elements are labeled. (C) Region of SAD-phased electron density at 1.5σ superimposed with the final model. (D) Cα trace of TRAF2 RZ_1 showing the zinc-coordinating residues. (E) Sequence alignment of TRAF2 from different species with TRAF3, TRAF5, and TRAF6: gray for zinc-coordinating residues, cyan for TRAF2 unique insertion, red for TRAF2 residues that would have clashed with Ubc13, green for TRAF2 dimerization interface residues, and yellow for residues in TRAF6 that contact Ubc13 and their equivalents in other TRAFs.

zinc finger in TRAF2. These structural differences prevent TRAF2 from interacting with Ubc13 and other related E2s. The structural observation should prompt a re-evaluation of the role of TRAF2 in TNFα signaling and may indicate that TRAF2-associated proteins such as cIAPs may be the ubiquitin ligases for NF-κB signaling.

Table 1: Crystallographic Statistics of TRAF2

structure determination	SAD
Data Collection	
beamlines	NSLS X4A
space group	$P6_522$
cell dimensions	
a, *b*, *c* (Å)	43.7, 43.7, 284.4
α, *β*, *γ* (deg)	90.0, 90.0, 120.0
resolution (Å)	1.9
R_{sym} (%)	7.0 (34.7)[a]
$I/\sigma I$	59.2 (4.0)[a]
completeness (%)	98.8 (90.1)[a]
redundancy	13.2 (5.6)[a]
Refinement	
resolution (Å)	37.8−1.9
no. of unique reflections	23319
R_{work}/R_{free} (%)	21.6/23.9
no. of atoms	
protein	940
water and ion	95
average *B* factor (Å^2)	
protein	36.5
water and ion	47.8
root-mean-square deviation	
bond lengths (Å)	0.004
angles (deg)	1.15
Ramachandran plot (%)	
most favored	87.6
allowed	100.0

[a]Data for the highest-resolution shell (1.97−1.90 Å) are given in parentheses.

EXPERIMENTAL PROCEDURES

Protein Expression, Purification, and Mutagenesis. We constructed the human TRAF2 construct RZ_1 (residues 1−133) with a C-terminal polyhistidine tag by cloning it into the pET26b vector (Novagen) using polymerase chain reaction (PCR) methods. The protein was expressed in BL21-CodonPlus(DE3) cells and purified by Ni affinity chromatography (Qiagen) followed by gel filtration chromatography (Superdex 200, GE Healthcare) in buffer containing 20 mM Tris-HCl (pH 7.5), 150 mM NaCl, and 5 mM dithiothreitol (DTT). Mutagenesis was performed with the QuikChange site-directed mutagenesis kit (Stratagene), and mutant proteins were expressed and purified similarly.

Crystallization and Structure Determination. Crystallization of TRAF2 RZ_1 was performed using sitting drop vapor diffusion at 20 °C. The crystallization condition included 10% PEG 8000, 0.1 M sodium Hepes (pH 7.5), and 8% ethylene glycol, and the crystallization drops contained a 1:1 protein: precipitant ratio. The diffraction data were collected at beamline X4A of the Brookhaven National Lab and processed using HKL2000 (*20*). The TRAF2 RZ_1 structure was determined by single-wavelength anomalous diffraction (SAD) (*21*) of the intrinsic zinc atoms using SOLVE and RESOLVE (*22*). The crystals belong to space group $P6_522$. Model building was performed in WinCoot (*23*). Refinement was achieved using CNS version 1.2 (*24*). Crystallographic statistics are listed in Table 1. All superpositions were performed with lsqman in the CCP4 suite (*25*). Structural presentations were generated using Pymol (DeLano Scientific).

Multiangle Light Scattering (*MALS*) *Analyses*. The molar masses of the WT and mutant TRAF2 RZ_1 were determined by MALS. The protein samples were injected into a Superdex 200 (10/300 GL) gel filtration column (GE Healthcare) equilibrated in a buffer containing 20 mM Tris (pH 7.5) and 150 mM NaCl. The chromatography system was coupled to a three-angle light scattering detector (mini-DAWN TRISTAR) and a refractive index detector (Optilab DSP) (Wyatt Technology). Data were collected every 0.5 s with a flow rate of 0.2 mL/min. Data analysis was conducted using ASTRA V.

In Vitro Ubiquitination Assays. In vitro ubiquitination assays with GST fusion proteins were performed essentially as described previously (*26*). TRAF2, TRAF3, TRAF5, and TRAF6 were expressed as GST fusion proteins in *Escherichia coli* and purified using glutathione−agarose beads (Sigma). The ubiquitination assay was performed in 20 *μ*L reaction volumes with the following components: glutathione−agarose bead-bound GST−TRAFs, 20 mM Hepes (pH 7.2), 10 mM $MgCl_2$, 1 mM DTT, 59 *μ*M His-ubiquitin, 50 nM E1, 850 nM E2, 1 mM ATP, 30 *μ*M creatine phosphate, and 1 unit of creatine kinase. The mixture was incubated at 37 °C for 2 h with gentle agitation. After incubation, 10 *μ*L of cold 20 mM Hepes (pH 7.4) was added to the reaction mixture, and samples were centrifuged for 20 min at 4 °C. A volume (20 *μ*L) of the supernatant was collected. The beads were washed, and both the beads and the supernatant were subjected to sodium dodecyl sulfate−polyacrylamide gel electrophoresis (SDS−PAGE) and immunoblotted with a ubiquitin-specific antibody [mouse anti-ubiquitin monoclonal (P4D1), Santa Cruz Biotechnology].

Transfection. TRAF2 and TRAF5 double-knockout MEFs were infected with empty retrovirus (pMX) or the indicated retrovirus expressing wild-type or mutant FLAG-tagged TRAF2 for 2 days and then selected for 2 weeks with puromycin (2 *μ*g/mL). Cells were plated in 10 cm dishes and starved overnight in incomplete medium. The cells were treated with TNFα (10 ng/mL) for the indicated times and harvested. Cell lysates were subjected to SDS−PAGE and immunoblotted with anti-FLAG (Sigma) and anti-phospho-I*κ*Bα antibodies (Cell Signaling).

RESULTS

Structure of the RING Domain and the First Zinc Finger (*RZ_1*) *of TRAF2*. The structure of TRAF2 RZ_1 (residues 1−133-His) was determined at 1.9 Å resolution using single-wavelength anomalous diffraction of the intrinsic zinc atoms (Table 1 and Figure 1B,C). The structure contains ordered residues from L14 to L133 and seven residues from the C-terminal His tag. The monomer structure seems rigid with extensive interactions with ∼660 Å^2 of buried surface area between the RING and the first zinc finger domains. The structure contains six α helices and five *β* strands. Among these, the RING region is composed of three α helices and three *β* strands while the zinc finger region contains two α helices and two *β* strands. A linker helix (α4) connects the two domains.

A DALI structural homology search (*27*) showed that the RING domain is similar to many known RING structures but is most similar to the RING domain of TRAF6 (*19*) with *Z* scores in the range of 7.1−7.6. A similar search using the first zinc finger of TRAF2 returned only the corresponding zinc finger of TRAF6 as a structural homologue with marginal *Z* scores of 2.6−2.9. To determine whether the relative structural arrangement between the RING domain and the first zinc finger has been observed before, we performed a structural homology search using both the RING and the first zinc finger structure of TRAF2. In addition to the top hits of TRAF6 with *Z* scores of 11.7−13.4, the

RAG1 dimerization domain has a *Z* score of 11.4 with TRAF2 and is the only known structure with a similar domain arrangement between a RING domain and a zinc finger. Interestingly, in addition to its role in RAG1 dimerization, the RING zinc finger structure of RAG1 also acts as a ubiquitin ligase (*28*).

Residues coordinating the two zinc atoms in the RING domain comprise the canonical RING signature motif, $CX_2CX_{(9-39)}CX_{(1-3)}HX_{(2-3)}CX_2CX_{(4-48)}CX_2C$ (where C is Cys, H is His, and X is any amino acid) (*29*) (Figure 1D,E). Similarly, the zinc figure is a classical CCHC type finger (Figure 1D,E). Although the current structure contains only the RING and the first zinc finger domains of TRAF2, zinc finger domains 2, 3, and 4 may be modeled on the basis of the conserved sequence spacing and structural relationship between the zinc fingers in all TRAF proteins (*19*).

TRAF2 RZ_1 Forms a Dimer in the Crystal and in Solution. There is only one monomer of TRAF2 RZ_1 in the crystallographic asymmetry unit. However, it forms a crystallographic dimer that is very similar to the RING dimer of TRAF6 (Figure 2A,B). The dimerization interface is formed mostly by residues Q46, F91, N94, A95, and R98, which all bury more than 50 $Å^2$ of surface area each. In particular, residue F91 buries 80 $Å^2$ of surface area, the most amount among all the interfacial residues (Figure 2C,D).

TRAF2 RZ_1 (molecular mass of 15.4 kDa) eluted at 16.6 mL on a Superdex 200 gel filtration column (Figure 2E), a position that is consistent with a dimer of TRAF2 based on the elution positions of gel filtration standards. The Q46A and N94A mutants both eluted at ~16.8 mL, mostly like wild-type TRAF2. The R98A mutant eluted at 17.2 mL, a significant shift from the wild-type position. The mutant that gave the most phenotype is F91A, which eluted at 17.4 mL, a position that is consistent with a monomer of TRAF2 RZ_1. Because gel filtration positions are affected by both size and shape and are not accurate indications of molecular mass, we further characterized the mutants using multiangle light scattering (MALS) in line with gel filtration chromatography. While TRAF2 RZ_1 gave a measured molecular mass of 26.7 kDa (3% error), which is consistent with a dimer, the F91A mutant exhibited a measured molecular mass of 16.1 kDa (5% error), which is consistent with mostly a monomer. The molecular mass measured by MALS for the R98A mutant is 25.1 kDa (3% error), showing that R98A produced only a weak defect in TRAF2 RZ_1 dimerization. These studies confirm that TRAF2 is a dimer both in the crystal and in solution and that this dimerization can be disrupted by a single mutation, F91A, at the observed interface.

To elucidate whether TRAF2 RING domain-mediated dimerization is important for its function, we reconstituted TRAF2 and TRAF5 double-knockout MEFs with WT and dimerization defective mutants of TRAF2. Surprisingly, WT TRAF2, the F91A mutant, and the double mutant (F91A/R98A) all successfully rescued TNFα-induced IκBα degradation, suggesting that TRAF2 dimerization is not critical for TNF signaling (Figure 2F). This observation is in contrast to the requirement for TRAF6 dimerization in IL-1 signaling (*19*). In TRAF6, its dimerization is crucial for its ubiquitin ligase activity. In this regard, one might argue that the lack of importance of TRAF2 dimerization is consistent with its apparent lack of E3 activity (see below).

Overall Structural Differences between TRAF2 and TRAF6. We performed structural superposition with TRAF6 using the RING alone, the zinc finger domain alone, or both domains of TRAF2. The cores of the RING domains of TRAF2 and TRAF6 are highly similar, with 56 aligned Cα positions and a 1.3 Å root-mean-square deviation (rmsd). There may be two regions of major differences (Figure 3A,B). The first difference is near the N-terminus in which an additional α helix (α1) of TRAF2 replaces the additional β strand (β1) in TRAF6. The second difference is at the TRAF2 unique insertion (Figure 1E). This insertion occurs immediately after the last coordinating Cys residue of the RING domain and contains nine residues. In the TRAF2 structure, this region forms an additional α helix (α3) followed by a loop. The zinc finger regions of TRAF2 and TRAF6 superimposed to 37 aligned Cα positions with a 1.4 Å rmsd. A gross difference in length and direction exists between helix α5 of TRAF2 and the corresponding helix in TRAF6 (Figure 3C). However, the zinc-coordinating residues are minimally affected (Figure 3C).

Although the RING and the zinc finger domains are individually similar between TRAF2 and TRAF6, there is a difference in the junction between the RING domain and the zinc finger. If both the RING domain and the zinc finger of TRAF2 are used for structural superposition with TRAF6, only 76 Cα positions can be aligned instead of the combined 93 (56 + 37) residues. The relative angular relationship between the RING domain and the zinc finger in TRAF2 is ~20° more acute than that in TRAF6 (Figure 3D,E). This difference is clearer when the zinc finger domain of TRAF2 is superimposed to the three consecutive zinc fingers of TRAF6 to represent the chain direction of TRAF2 in the second and third zinc fingers. The conformational difference may be due to the different interdomain interaction; in particular, the interaction between the β1 strand of the RING domain and the β2 and β3 strands of the zinc finger in TRAF6 is replaced by the interaction between helix α1 of the RING domain and the same region of the zinc finger in TRAF2 (Figure 3A).

Multifaceted Differences Underlie the Lack of Ubc13 Interaction in TRAF2. We have shown earlier that unlike TRAF6, TRAF2 did not interact with Ubc13 in a yeast two-hybrid assay (*19*). Indeed, while the TRAF6 RING domain and the first zinc finger construct is sufficient for Ubc13 interaction (*19*), the same region of TRAF2 did not interact with Ubc13 on a native PAGE assay (Figure 4A).

Structural analysis revealed that this lack of Ubc13 interaction might be a consequence of multiple factors. First, if a complex of TRAF2 with Ubc13 is constructed using the known TRAF6−Ubc13 interaction (*19*), two regions of the TRAF2 structure would sterically clash with Ubc13 (<2 Å interatomic distances) (Figure 4B). One region is from the N-terminus, comprising residues Q16, G18, and K21. The other region is from the TRAF2 unique insertion and composed of residues A70 and H74. Second, core residues at the Ubc13-interacting site of TRAF6 are completely different in TRAF2 (Figures 1E and 4C). Specifically, residues E69, P71, I72, L74, M75, A101, and P106 are changed to L33, S35, A36, R38, N39, G65, and A70, respectively. These residues mainly exhibit side chain differences with fairly conserved main chain conformations. Third, both the sequence and conformation of residues near the N-terminus for Ubc13 interaction in TRAF6 are different in TRAF2 (Figure 4D). The difference in conformation is likely because of the two consecutive Pro residues (P62 and P63) in TRAF6 and no Pro residues in TRAF2 in this region. In addition, TRAF6 residues in direct contact with Ubc13, Q54 and D57, are replaced with P17 and S20, respectively.

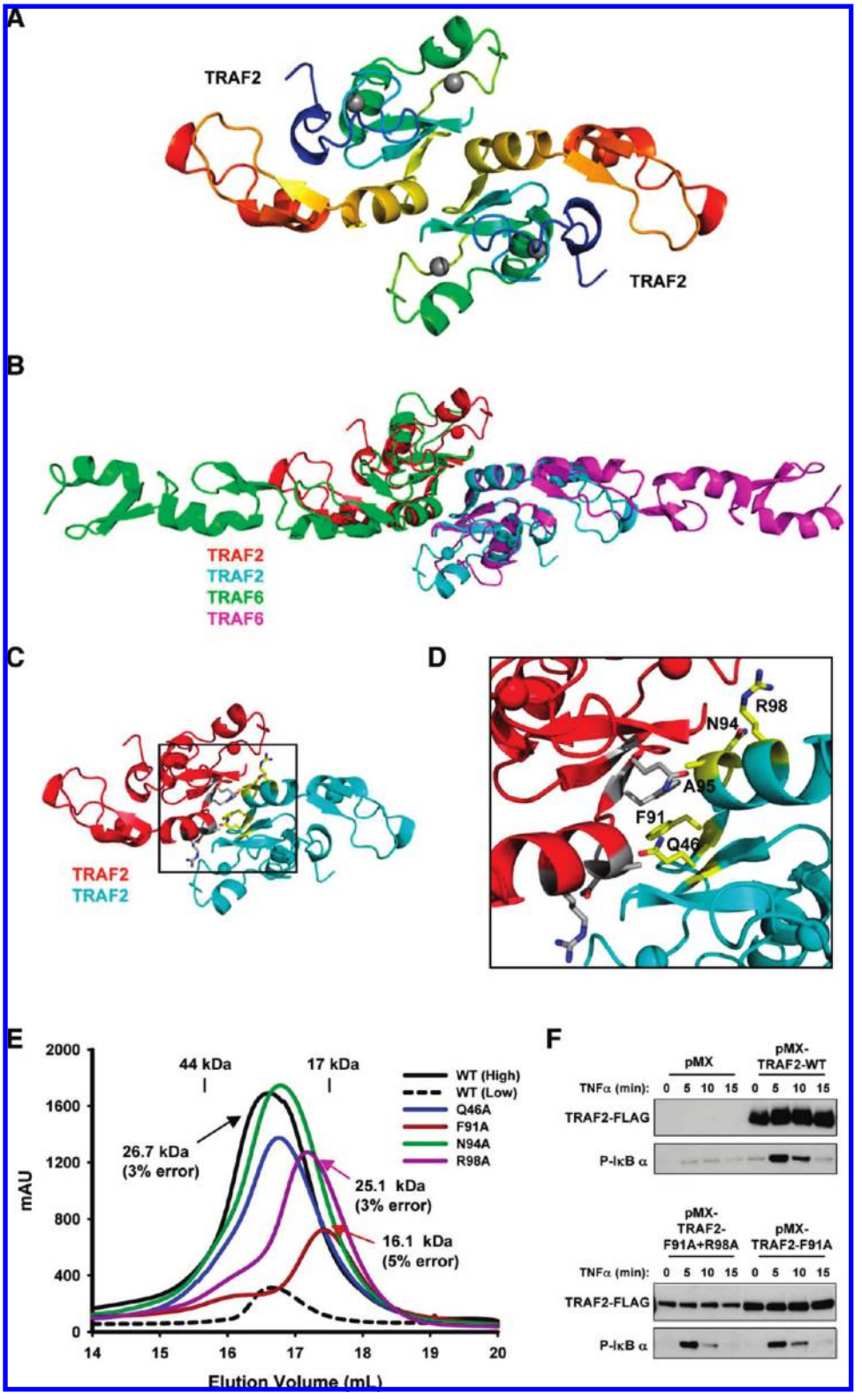

FIGURE 2: TRAF2 dimerization in the crystal and in solution. (A) TRAF2 RZ_1 dimer shown in a ribbon diagram colored in a rainbow mode. (B) Superposition of the TRAF2 RZ_1 dimer (red and cyan) with the TRAF6 RZ_{123} dimer (Protein Data Bank entry 3HCS, magenta and green). (C) TRAF2 RZ_1 dimer shown with residues at the dimerization interface. The region that is shown in detail in panel D is blocked by a rectangle. (D) Details of the TRAF2 dimerization interaction. Critical residues are labeled on one side of the symmetrical interface. (E) Superposition of gel filtration profiles of WT TRAF2 RZ_1 (high, at higher concentrations; low, at lower concentrations) and Q46A, F91A, N94A, and R98A mutants of TRAF2 RZ_1. MALS measurement results for WT TRAF2 RZ_1, the F91A mutant, and the R98A mutant, as well as elution positions of molecular mass standards, are shown. (F) TRAF2 RING domain dimerization mutants rescued TNFα-induced IκBα phosphorylation in TRAF2 and TRAF5 double-knockout MEFs.

TRAF2 Failed To Interact with a Number of Other E2s. The inability of TRAF2 to interact with Ubc13 is intriguing considering that TRAF2 is crucial for TNFα-induced NF-κB activation. One possibility is that TRAF2 uses another E2 to perform K63-linked polyubiquitination. In this regard, at least UbcH5 has been implicated in mediating both K48- and

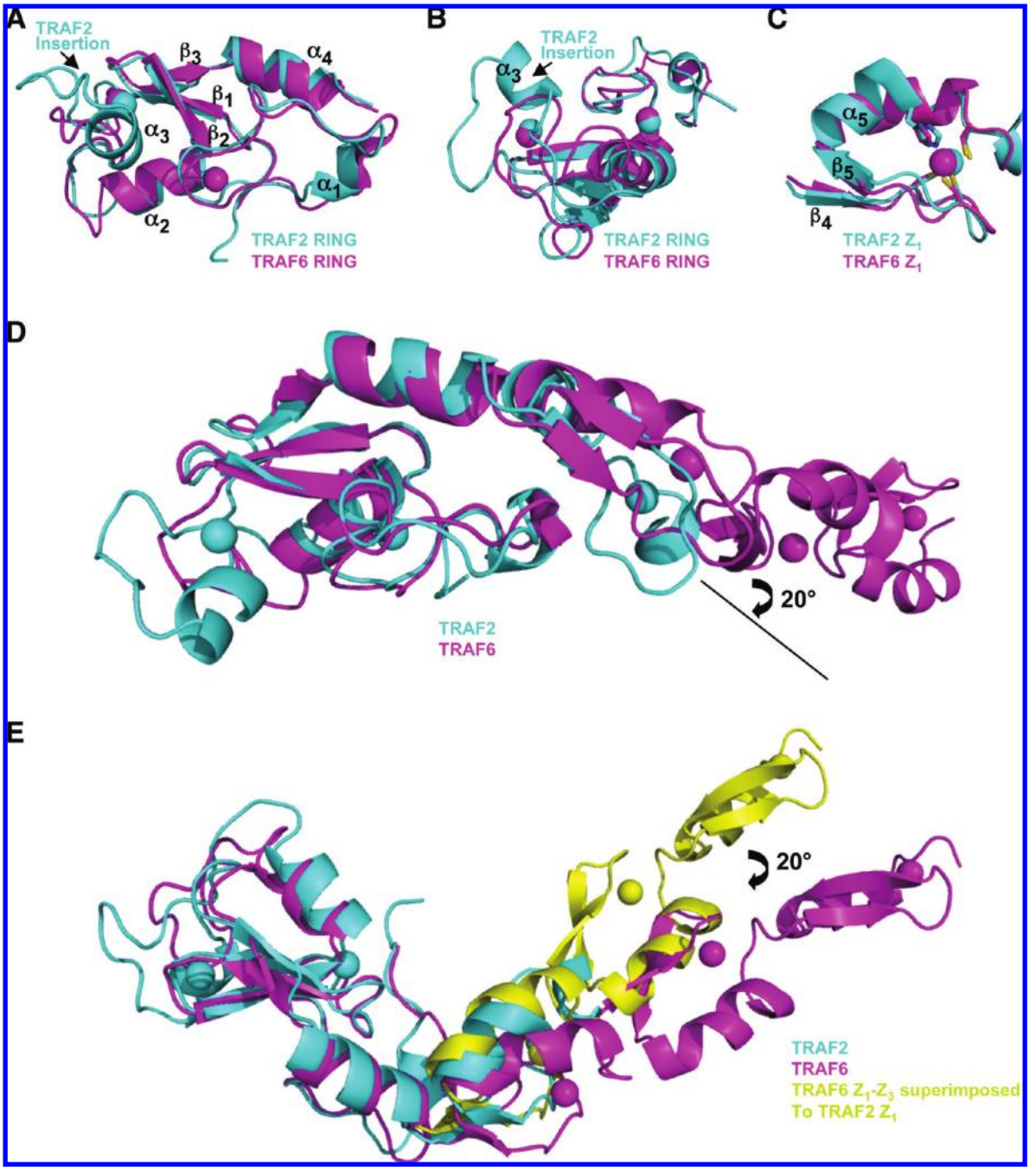

FIGURE 3: Comparison between TRAF2 RZ_1 (cyan) and TRAF6 RZ_{123} (magenta). (A and B) Superposition of TRAF2 and TRAF6 RING domains, showing the location of the unique insertion of TRAF2 in two roughly orthogonal orientations. (C) Superposition of the first zinc finger domains of TRAF2 and TRAF6. (D and E) Superposition of TRAF2 RZ_1 with TRAF6 RZ_{123}, showing the difference in relative orientation of the zinc finger domain relative to the RING domain. (E) Z_1-Z_3 domains of TRAF6 superimposed onto Z_1 of TRAF2 to show more clearly the relative rotation of ~20°.

K63-linked polyubiquitination (*30*). However, structurally UbcH5 is very similar to Ubc13 (Figure 4E), and the same steric hindrance between TRAF2 and Ubc13 should be true for UbcH5. This would then disallow TRAF2 to interact with UbcH5. To confirm our hypothesis and to test the ability of TRAF2 to cooperate with additional E2s, we performed in vitro polyubiquitination assays using full-length TRAF2 and eight other E2s (Figure 5A). While TRAF6 also promoted polyubiquitin chain synthesis by UbcH5a, UbcH5b, UbcH5c, and UbcH6, TRAF2, as well as TRAF3 and TRAF5, failed to generate polyubiquitin chains in the presence of any of the tested E2s. In contrast to the lack of E3 activity of TRAF2, both purified cIAP1 and cIAP2 can undergo autoubiquitination (Figure 5B).

DISCUSSION

The data presented here support the possibility that TRAF2 per se is not a ubiquitin ligase. Nonetheless, we cannot rule out the possibility that TRAF2 may become an active E3 after undergoing post-translational modifications. In fact, it has been shown that residue T117 of TRAF2 is phosphorylated by PKCδ following TNFα stimulation and this phosphorylation is required for TRAF2 functional activity (*31*). However, when we generated the phospho-mimic mutant T117E or the

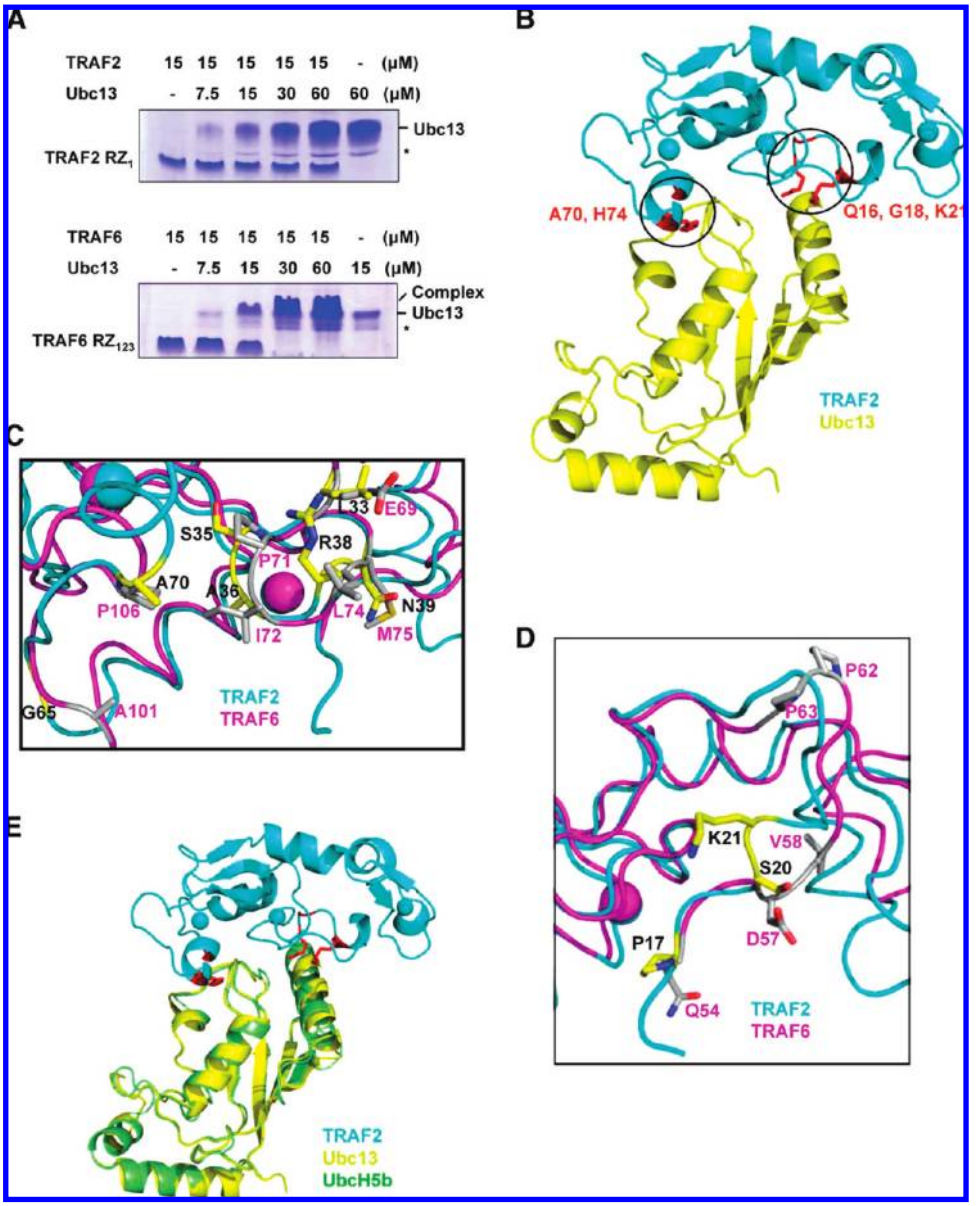

FIGURE 4: Lack of interaction between TRAF2 and E2s. (A) Native PAGE of TRAF2 RZ_1 with Ubc13 using an 8 to 25% gradient PhastGel on a PhastSystem (GE Healthcare). A similar native PAGE of TRAF6 RZ_{123} with Ubc13 is shown as a positive control. The gels were stained with Coomassie blue. (B) TRAF2 residues (red) that would have sterically clashed with Ubc13 if the interaction were to follow the mode of the TRAF6−Ubc13 interaction (Protein Data Bank entry 3HCU). (C) Close-up view of the superposition of the RING domains of TRAF2 (cyan) and TRAF6 (magenta). TRAF6 residues in direct contact with Ubc13 and their equivalents for TRAF2 are colored yellow for TRAF2 and gray for TRAF6. (D) Conformational difference in the region immediately preceding the RING domain between TRAF2 and TRAF6. (E) Superposition of UbcH5b (Protein Data Bank entry 2CLW) onto the hypothetical TRAF2−Ubc13 complex, showing that the TRAF2 residues that clash with Ubc13 would have clashed with Ubc5Hb as well.

phospho-disabling mutant T117A or used recombinant PKCδ to phosphorylate wild-type TRAF2 and these mutants, we could not observe any activity of these TRAF2 variants in promoting polyubiquitin chain synthesis or autoubiquitination by the Ubc13−Uev1A complex (data not shown).

Is there a sequence signature that distinguishes RING domain type E3s from RING proteins with no E3 activities? Recently, a genomewide analysis of human E2−E3 interactions using yeast two-hybrid screens identified two sequence positions that correspond to A36 and I61 of TRAF2 as being critical (*32*). In most E3s, these positions are Ile and Trp, respectively. However, this sequence conservation is not strict; for example, in TRAF6, these are Ile and Ser, respectively. Instead, it appears that sequence signatures for the RING domain with E3 activities are complex, for which a better prediction might be achieved through three-dimensional homology modeling and free energy calculations for the E2−E3 pairs (*32*).

It seems more likely that TRAF2-associated proteins might be functioning as ubiquitin ligases for the TNF receptor superfamily pathways. TRAF2 has been known to be constitutively associated with cIAP1 and cIAP2, members of the inhibitor of apoptosis (IAP) family (*33*). Neither cIAP1 nor cIAP2 appears to be potent in caspase inhibition (*34*). Alternatively, cIAP1 and cIAP2 are RING domain-containing proteins and known to promote K48-linked polyubiquitination (*35*). It has also been shown that cIAP1 and cIAP2 facilitate cancer cell survival by functioning as ubiquitin ligases that promote RIP1 ubiquitination (*36*).

The sequences of the RING domains of cIAP1 and cIAP2 suggest that they might be able to interact with Ubc13 (*19*) and

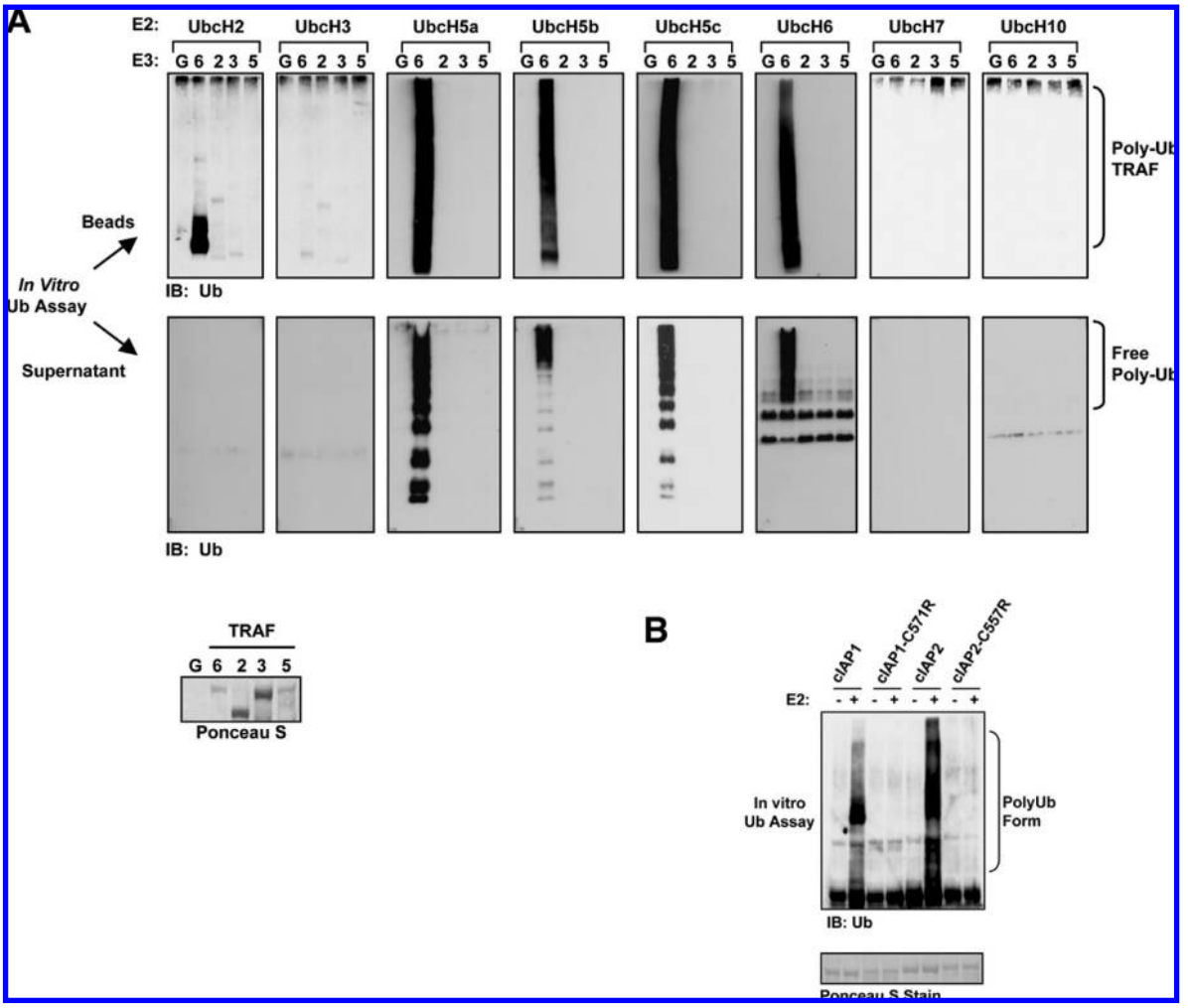

FIGURE 5: Ubiquitination assays. (A) Autoubiquitination and free chain polyubiquitin synthesis in vitro by TRAF2, TRAF3, TRAF5, and TRAF6 with a series of E2s. The indicated GST fusion proteins bound to glutathione−agarose beads were subjected to an in vitro ubiquitination assay in the presence of the indicated E2s. Following the ubiquitination assay, a portion of the supernatant was subjected to SDS−PAGE and immunoblotted with anti-ubiquitin (middle panels). The beads were washed, subjected to SDS−PAGE, and immunoblotted with anti-ubiquitin (top panels). The membranes were stained with Ponceau S, and one representative membrane is shown (bottom panel): G, GST; 6, GST−TRAF6; 2, GST−TRAF2; 3, GST−TRAF3; 5, GST−TRAF5. (B) cIAP1 and cIAP2 undergo RING domain-dependent autoubiquitination in the presence of the Ubc13−Uev1A E2 complex: C571R, RING domain mutant of cIAP1; C557R, RING domain mutant of cIAP2.

therefore might be able to promote K63-linked polyubiquitination as well. Indeed, we could demonstrate Ubc13−Uev1A complex-dependent autopolyubiquitination of cIAP1 and cIAP2. The zinc-coordinating residues in cIAP1 and cIAP2 are critical for this polyubiquitination. These data suggest that cIAPs may be able to serve as the E3s for K63-linked polyubiquitination and NF-κB activation in TRAF2 signaling pathways. Our in vitro observation is consistent with earlier studies showing the role of cIAPs in formation of the TNF receptor signaling complex and NF-κB activation (*37*). More convincingly, when both cIAP1 and cIAP2 are absent, RIP1 polyubiquitination was inhibited with a reduced level of phosphorylation of IKKβ (*38*).

In this context, one of the major roles of TRAF2 is to recruit cIAP1 and cIAP2. The interaction between TRAF2 and cIAPs is direct, as shown by both earlier yeast two-hybrid studies (*33*) and our unpublished results using purified TRAF2 and the cIAP2 BIR1 domain. In one likely scenario, the association of cIAPs with TRAF2 brings cIAPs to the TNF receptor signaling complex for activation of the canonical NF-κB signaling pathway through RIP1 ubiquitination (*38*). In another more clearly defined scenario in the role of cIAPs in suppressing the non-canonical NF-κB pathway by ubiquitinating the kinase NIK, TRAF2 is absolutely required for this activity of cIAPs. It is the bridge that brings cIAPs to its substrate NIK by interacting with TRAF3 that in turn associates with NIK (*39*). TRAF2 itself is also a substrate of cIAPs (*40*). In the absence of appropriate substrates or in the presence of IAP antagonists, cIAPs can also undergo autoubiquitination and degradation (*35*, *41*, *42*). It is possible that in the multiprotein complex, TRAF2 functions to alter the substrate specificity and perhaps also the ubiquitination efficiency of cIAPs. The latter has also been proposed as the role of chain elongation factors or E4s (*14*). It is possible that cIAPs are just one of the E3s in the TRAF2 signaling pathways.

If TRAF2 is not an E3, but rather a platform for recruiting cIAP1 and cIAP2 via other domains of TRAF2, what is the function of its RING domain? It has long been observed that RING domain deletion converts TRAF2 from a positive regulator of NF-κB signaling to a dominant negative inhibitor (*1*). There may be at least a couple of possible answers for this question. The TRAF2 RING domain may function as a K63-linked polyubiquitination acceptor site, rather than an E3. This site has been mapped to K31 in its RING domain (*43*). Perhaps another quite plausible possibility lies in the requirement of the TRAF2 RING domain for the translocation of TNF receptor

family signaling complexes to membrane rafts, a process required for their signaling (*44*). In any case, the structural incompatibility of the TRAF2 RING domain for interacting with Ubc13-like E2s should prompt a re-evaluation of its role in signal transduction.

ACKNOWLEDGMENT

We thank Randy Abramowitz and John Schwanof for data collection at beamline X4A of NSLS, PXRR staff for data collection at beamline X29 of NSLS, Jin Wu for maintaining X-ray and computer equipment, and Dr. H. Nakano for the TRAF2 and TRAF5 double-knockout MEFs.

REFERENCES

1. Rothe, M., Wong, S. C., Henzel, W. J., and Goeddel, D. V. (1994) A novel family of putative signal transducers associated with the cytoplasmic domain of the 75 kDa tumor necrosis factor receptor. *Cell 78*, 681–692.
2. Chung, J. Y., Lu, M., Yin, Q., and Wu, H. (2007) Structural revelations of TRAF2 function in TNF receptor signaling pathway. *Adv. Exp. Med. Biol. 597*, 93–113.
3. Wajant, H., Henkler, F., and Scheurich, P. (2001) The TNF-receptor-associated factor family: Scaffold molecules for cytokine receptors, kinases and their regulators. *Cell. Signalling 13*, 389–400.
4. Wu, H. (2004) Assembly of post-receptor signaling complexes for the tumor necrosis factor receptor superfamily. *Adv. Protein Chem. 68*, 225–279.
5. Pineda, G., Ea, C. K., and Chen, Z. J. (2007) Ubiquitination and TRAF signaling. *Adv. Exp. Med. Biol. 597*, 80–92.
6. Park, Y. C., Burkitt, V., Villa, A. R., Tong, L., and Wu, H. (1999) Structural basis for self-association and receptor recognition of human TRAF2. *Nature 398*, 533–538.
7. McWhirter, S. M., Pullen, S. S., Holton, J. M., Crute, J. J., Kehry, M. R., and Alber, T. (1999) Crystallographic analysis of CD40 recognition and signaling by human TRAF2. *Proc. Natl. Acad. Sci. U.S.A. 96*, 8408–8413.
8. Park, Y. C., Ye, H., Hsia, C., Segal, D., Rich, R. L., Liou, H.-L., Myszka, D. G., and Wu, H. (2000) A novel mechanism of TRAF signaling revealed by structural and functional analyses of the TRADD-TRAF2 interaction. *Cell 101*, 777–787.
9. Ni, C. Z., Welsh, K., Leo, E., Chiou, C. K., Wu, H., Reed, J. C., and Ely, K. R. (2000) Molecular basis for CD40 signaling mediated by TRAF3. *Proc. Natl. Acad. Sci. U.S.A. 97*, 10395–10399.
10. Ye, H., Arron, J. R., Lamothe, B., Cirilli, M., Kobayashi, T., Shevde, N. K., Segal, D., Dzivenu, O. K., Vologodskaia, M., Yim, M., Du, K., Singh, S., Pike, J. W., Darnay, B. G., Choi, Y., and Wu, H. (2002) Distinct molecular mechanism for initiating TRAF6 signalling. *Nature 418*, 443–447.
11. Deng, L., Wang, C., Spencer, E., Yang, L., Braun, A., You, J., Slaughter, C., Pickart, C., and Chen, Z. J. (2000) Activation of the IκB kinase complex by TRAF6 requires a dimeric ubiquitin-conjugating enzyme complex and a unique polyubiquitin chain. *Cell 103*, 351–361.
12. Pickart, C. M., and Eddins, M. J. (2004) Ubiquitin: Structures, functions, mechanisms. *Biochim. Biophys. Acta 1695*, 55–72.
13. Pickart, C. M., and Fushman, D. (2004) Polyubiquitin chains: Polymeric protein signals. *Curr. Opin. Chem. Biol. 8*, 610–616.
14. Hochstrasser, M. (2006) Lingering mysteries of ubiquitin-chain assembly. *Cell 124*, 27–34.
15. Dye, B. T., and Schulman, B. A. (2007) Structural mechanisms underlying posttranslational modification by ubiquitin-like proteins. *Annu. Rev. Biophys. Biomol. Struct. 36*, 131–150.
16. Wu, C. J., Conze, D. B., Li, T., Srinivasula, S. M., and Ashwell, J. D. (2006) Sensing of Lys 63-linked polyubiquitination by NEMO is a key event in NF-κB activation [corrected]. *Nat. Cell Biol. 8*, 398–406.
17. Ea, C. K., Deng, L., Xia, Z. P., Pineda, G., and Chen, Z. J. (2006) Activation of IKK by TNFα requires site-specific ubiquitination of RIP1 and polyubiquitin binding by NEMO. *Mol. Cell 22*, 245–257.
18. Kelliher, M. A., Grimm, S., Ishida, Y., Kuo, F., Stanger, B. Z., and Leder, P. (1998) The death-domain kinase RIP mediates the TNF-induced NF-kB signal. *Immunity 8*, 297–303.
19. Yin, Q., Lin, S. C., Lamothe, B., Lu, M., Lo, Y. C., Hura, G., Zheng, L., Rich, R., Campos, A. D., Myszka, D. G., Lenardo, M. J., Darnay, B. G., and Wu, H. (2009) E2 interaction and dimerization in the crystal structure of TRAF6. *Nat. Struct. Mol. Biol. 16*, 658–666.
20. Otwinowski, Z., and Minor, W. (1997) Processing of X-ray diffraction data collected in oscillation mode. *Methods Enzymol. 276*, 307–326.
21. Hendrickson, W. A. (1985) Analysis of protein structures from diffraction measurements at multiple wavelengths. *Trans. Am. Crystallogr. Assoc. 21*, 11.
22. Terwilliger, T. (2004) SOLVE and RESOLVE: Automated structure solution, density modification and model building. *J. Synchrotron Radiat. 11*, 49–52.
23. Emsley, P., and Cowtan, K. (2004) Coot: Model-building tools for molecular graphics. *Acta Crystallogr. D60*, 2126–2132.
24. Brunger, A. T., Adams, P. D., Clore, G. M., DeLano, W. L., Gros, P., Grosse-Kunstleve, R. W., Jiang, J. S., Kuszewski, J., Nilges, M., Pannu, N. S., Read, R. J., Rice, L. M., Simonson, T., and Warren, G. L. (1998) Crystallography & NMR system: A new software suite for macromolecular structure determination. *Acta Crystallogr. D54*, 905–921.
25. Collaborative Computational Project, No. 4 (1994) The CCP4 Suite: Programs for Protein Crystallography. *Acta Crystallogr. D50*, 760–763.
26. Lamothe, B., Besse, A., Campos, A. D., Webster, W. K., Wu, H., and Darnay, B. G. (2007) Site-specific Lys-63-linked tumor necrosis factor receptor-associated factor 6 auto-ubiquitination is a critical determinant of IκB kinase activation. *J. Biol. Chem. 282*, 4102–4112.
27. Holm, L., and Sander, C. (1995) Dali: A network tool for protein structure comparison. *Trends Biochem. Sci. 20*, 478–480.
28. Yurchenko, V., Xue, Z., and Sadofsky, M. (2003) The RAG1 N-terminal domain is an E3 ubiquitin ligase. *Genes Dev. 17*, 581–585.
29. Deshaies, R. J., and Joazeiro, C. A. (2009) RING domain E3 ubiquitin ligases. *Annu. Rev. Biochem. 78*, 399–434.
30. Brzovic, P. S., and Klevit, R. E. (2006) Ubiquitin transfer from the E2 perspective: Why is UbcH5 so promiscuous? *Cell Cycle 5*, 2867–2873.
31. Li, S., Wang, L., Berman, M. A., Zhang, Y., and Dorf, M. E. (2006) RNAi screen in mouse astrocytes identifies phosphatases that regulate NF-κB signaling. *Mol. Cell 24*, 497–509.
32. Markson, G., Kiel, C., Hyde, R., Brown, S., Charalabous, P., Bremm, A., Semple, J., Woodsmith, J., Duley, S., Salehi-Ashtiani, K., Vidal, M., Komander, D., Serrano, L., Lehner, P., and Sanderson, C. M. (2009) Analysis of the human E2 ubiquitin conjugating enzyme protein interaction network. *Genome Res. 19*, 1905–1911.
33. Rothe, M., Pan, M. G., Henzel, W. J., Ayres, T. M., and Goeddel, D. V. (1995) The TNFR2-TRAF signaling complex contains two novel proteins related to baculoviral inhibitor of apoptosis proteins. *Cell 83*, 1243–1252.
34. Eckelman, B. P., and Salvesen, G. S. (2006) The human anti-apoptotic proteins cIAP1 and cIAP2 bind but do not inhibit caspases. *J. Biol. Chem. 281*, 3254–3260.
35. Varfolomeev, E., Blankenship, J. W., Wayson, S. M., Fedorova, A. V., Kayagaki, N., Garg, P., Zobel, K., Dynek, J. N., Elliott, L. O., Wallweber, H. J., Flygare, J. A., Fairbrother, W. J., Deshayes, K., Dixit, V. M., and Vucic, D. (2007) IAP antagonists induce autoubiquitination of c-IAPs, NF-κB activation, and TNFα-dependent apoptosis. *Cell 131*, 669–681.
36. Bertrand, M. J., Milutinovic, S., Dickson, K. M., Ho, W. C., Boudreault, A., Durkin, J., Gillard, J. W., Jaquith, J. B., Morris, S. J., and Barker, P. A. (2008) cIAP1 and cIAP2 facilitate cancer cell survival by functioning as E3 ligases that promote RIP1 ubiquitination. *Mol. Cell 30*, 689–700.
37. Santoro, M. M., Samuel, T., Mitchell, T., Reed, J. C., and Stainier, D. Y. (2007) Birc2 (cIap1) regulates endothelial cell integrity and blood vessel homeostasis. *Nat. Genet. 39*, 1397–1402.
38. Mahoney, D. J., Cheung, H. H., Mrad, R. L., Plenchette, S., Simard, C., Enwere, E., Arora, V., Mak, T. W., Lacasse, E. C., Waring, J., and Korneluk, R. G. (2008) Both cIAP1 and cIAP2 regulate TNFα-mediated NF-κB activation. *Proc. Natl. Acad. Sci. U.S.A. 105*, 11778–11783.
39. Zarnegar, B. J., Wang, Y., Mahoney, D. J., Dempsey, P. W., Cheung, H. H., He, J., Shiba, T., Yang, X., Yeh, W. C., Mak, T. W., Korneluk, R. G., and Cheng, G. (2008) Noncanonical NF-κB activation requires coordinated assembly of a regulatory complex of the adaptors cIAP1, cIAP2, TRAF2 and TRAF3 and the kinase NIK. *Nat. Immunol. 9*, 1371–1378.
40. Dupoux, A., Cartier, J., Cathelin, S., Filomenko, R., Solary, E., and Dubrez-Daloz, L. (2009) cIAP1-dependent TRAF2 degradation regulates the differentiation of monocytes into macrophages and their response to CD40 ligand. *Blood 113*, 175–185.
41. Vince, J. E., Wong, W. W., Khan, N., Feltham, R., Chau, D., Ahmed, A. U., Benetatos, C. A., Chunduru, S. K., Condon, S. M., McKinlay, M., Brink, R., Leverkus, M., Tergaonkar, V., Schneider, P., Callus, B. A.,

Koentgen, F., Vaux, D. L., and Silke, J. (2007) IAP antagonists target cIAP1 to induce TNFα-dependent apoptosis. *Cell 131*, 682–693.

42. Petersen, S. L., Wang, L., Yalcin-Chin, A., Li, L., Peyton, M., Minna, J., Harran, P., and Wang, X. (2007) Autocrine TNFα signaling renders human cancer cells susceptible to Smac-mimetic-induced apoptosis. *Cancer Cell 12*, 445–456.
43. Li, S., Wang, L., and Dorf, M. E. (2009) PKC phosphorylation of TRAF2 mediates IKKα/β recruitment and K63-linked polyubiquitination. *Mol. Cell 33*, 30–42.
44. Arron, J. R., Pewzner-Jung, Y., Walsh, M. C., Kobayashi, T., and Choi, Y. (2002) Regulation of the subcellular localization of tumor necrosis factor receptor-associated factor $(TRAF)_2$ by TRAF1 reveals mechanisms of TRAF2 signaling. *J. Exp. Med. 196*, 923–934.